



OPEN ACCESS

EDITED BY
Urszula Jelen,
Genesis Care, Australia

REVIEWED BY
Danilo Maziero,
University of California, United States
Michael Martyn,
Galway Clinic, Ireland

*CORRESPONDENCE
Justine M. Cunningham,
jcunnin5@hfhs.org

SPECIALTY SECTION
This article was submitted to Medical
Physics and Imaging,
a section of the journal
Frontiers in Physics

RECEIVED 24 February 2022
ACCEPTED 28 July 2022
PUBLISHED 29 August 2022

CITATION
Cunningham JM, Chin Snyder K, Kim JP,
Siddiqui SM, Parikh P, Chetty IJ and
Dolan JL (2022), On-line adaptive and
real-time intrafraction motion
management of spine-SBRT on an MR-
linac.
Front. Phys. 10:882564.
doi: 10.3389/fphy.2022.882564

COPYRIGHT
© 2022 Cunningham, Chin Snyder, Kim,
Siddiqui, Parikh, Chetty and Dolan. This
is an open-access article distributed
under the terms of the [Creative
Commons Attribution License \(CC BY\)](https://creativecommons.org/licenses/by/4.0/).
The use, distribution or reproduction in
other forums is permitted, provided the
original author(s) and the copyright
owner(s) are credited and that the
original publication in this journal is
cited, in accordance with accepted
academic practice. No use, distribution
or reproduction is permitted which does
not comply with these terms.

On-line adaptive and real-time intrafraction motion management of spine-SBRT on an MR-linac

Justine M. Cunningham*, Karen Chin Snyder, Joshua P. Kim, Salim M. Siddiqui, Parag Parikh, Indrin J. Chetty and Jennifer L. Dolan

Department of Radiation Oncology, Henry Ford Cancer Institute, Detroit, MI, United States

Purpose: The superior soft-tissue contrast of MRI-guided radiotherapy offers enhanced localization accuracy of the spinal cord in spine Stereotactic Body Radiotherapy (SBRT). This work includes a planning study for spine-SBRT on an MR-Linac. Additionally, a patient with spine metastasis was treated using an adaptive radiation therapy workflow. We report our initial experience of targeting accuracy, image-guided localization, on-line adaptive planning, and treatment with real-time intrafraction imaging with automatic beam gating.

Methods: Six spine-SBRT patients were retrospectively re-planned to 18 Gy in 1-fraction on a commercial, Monte Carlo-based MR-Linac treatment planning system. Plans were generated using 9–13 step-and-shoot intensity-modulated radiation therapy 6 MV-flattening filter free beams and optimized to achieve plan quality criteria recommended by RTOG-0631. One thoracic vertebral body clinical case was treated to 27 Gy in 3-fractions utilizing ART, where daily anatomical changes were accounted for via re-planning and treatment in an on-line manner to account for limited ability to correct rotational setup uncertainties.

Results: Plans met all critical-tissue constraints outlined in RTOG-0631 and AAPM Task Group-101, while covering 90% of the target with the prescription dose. Clinically, visibility of the spinal cord allowed for patient setup focusing on spinal cord-alignment. Utilization of the online ART workflow, while re-contouring the target and spinal cord, enabled an increase in prescription dose coverage from 89 to 95% in two of three fractions while maintaining acceptable doses to organs-at-risk. Real-time MR-cine imaging demonstrated sufficient quality for the automatic beam gating algorithm to provide intrafraction motion management of the spinal canal utilizing a 3.0 mm gating boundary and 1–2% region of excursion allowance, in the sagittal plane. A decrease in coverage, below the 95% threshold was noted in post-treatment volumetric imaging due to lateral movement not observed during real-time gating.

Conclusion: Achieved plan quality and deliverability was within accepted standards. MR-guidance with an on-line ART workflow offered increased accuracy in the localization of the spinal cord at the time of treatment to

enhance both tissue sparing and target volume coverage. Increased spatial resolution of cine-images, and tracking in three-dimensions would be beneficial for future spine-SBRT treatments on the MR-Linac.

KEYWORDS

MR-linac, spine, SBRT (stereotactic body radiation therapy), adaptive, IGRT (image guided radiation therapy), SRS (stereotactic radiosurgery)

Introduction

Stereotactic Body Radiotherapy (SBRT) to previously untreated spinal metastases is linked to low rates of serious adverse events, while achieving favorable rates of complete pain response (approximately 50%) and local control (approximately 90% at 1 year) [1]. Spine SBRT relies on superior patient positioning techniques to enable confidence in the delivery of escalated dose [2]. Additionally, delineation of the targeted patient anatomy often relies on diagnostic magnetic resonance imaging (MRI) scans, which must be registered to a treatment planning computed tomography (CT) image, adding associated registration uncertainties in target definition [3, 4]. MRI-guided linear accelerators (MR-Linacs) can increase the targeting accuracy and safety of spine-SBRT treatments by allowing for visualization of soft-tissue features that are used to define the treatment volumes and organs at risk (OARs) for planning and localization for patient treatments [5]. Due to the MR simulation images acquired on the treatment machine, variables such as patient position and slice thickness can be optimized to minimize co-registration errors [6].

For spine-SBRT cases, the location of the spinal cord relative to the vertebral body and epidural involvement is crucial to the success of the planning and delivery process [7]. Traditionally, spine-SBRT patients are treated on Linacs with CT-based on-board imaging. Patient positioning at the time of treatment then relies on the bony anatomy that is visible on both the treatment planning CT and x-ray based on-board imaging (cone-beam CTs or planar imaging) as a surrogate for the specific tissues that are targeted [2, 8]. MRI-guided radiation therapy (MRgRT) offers the benefit of increased soft-tissue contrast [5], which may improve localization of the spinal cord and involved soft tissue for spine SBRT at the time of treatment. Differences in patient localization have been observed when aligning to bony anatomy as a surrogate as opposed to the spinal cord itself [9]. Additionally, visibility of the spinal canal in MR sagittal cine imaging, may allow for spinal canal based real-time gated treatments to account for movement during treatment.

To assess the potential advantages that MR-Linacs can provide to spine-SBRT treatments, this work includes a treatment-plan quality and deliverability study for a set of spine-SBRT plans retrospectively generated on an MR-Linac. Previous studies have shown that MRgRT has the ability to provide plans of similar quality to conventional spine-SBRT treatment plans utilizing Volumetric Modulated Arc Therapy

(VMAT) [10, 11]. However, the robustness of the planning technique was not demonstrated throughout an adaptive radiation therapy (ART) workflow, where the location of the spinal cord relative to the vertebral body may vary [12–14].

Current literature outlines the possible advantages of MRgRT in spine-SBRT, including target delineation, co-registration errors and adaptive planning, specifically related to accounting for variation in bowel positioning [6, 15]. A previous article includes a review of two adaptive approaches for spine-SBRT, including “adapt to position” and “adapt to shape” workflows. The “adapt to position” workflow corrects for translational shifts by adjusting beam geometry without additional structure delineation. The “adapt to shape” workflow allows for re-contouring and re-optimization to account for interfraction changes, however in the case presented the target contour was rigidly copied, without reference to additional adjustments to the target or spinal cord contour [15]. Studies have shown that the spinal cord can move with respect to rigid bony anatomy during treatment with median bulk displacements greater than 0.5 mm and maximal displacements greater than 2.2 mm in each direction [12, 13]. Where these displacements may result in potentially detrimental dose effects to the spinal cord [14]. Additionally, current MRgRT machines are limited to three degrees-of-freedom (DoF) couch corrections, where the inability to correct for rotational setup errors has been shown to result in reduced prescription dose coverage of the target [16, 17]. To account for this moving spinal cord and under-coverage in dose to the target, we propose an ART workflow allowing for re-contouring and re-optimization to account for interfraction anatomical and setup variations. This paper focuses on the clinical workflow followed to clinically treat a patient with oligometastatic disease of the spine using an on-line ART workflow for spine-SBRT. Here we report on our initial experience of targeting accuracy, image-guided localization, and treatment delivery. We report the results of the target dose coverage and normal tissue doses achieved during adaptation for several treatment fractions. We also present the results of intrafraction real-time gating of the spinal canal utilizing MR cine imaging. To our knowledge, this is the first report of the workflow required for online adaptive MRgRT for treatment of metastatic spinal cord lesions, demonstrating the potential need for on-table adaptation in this treatment setting. Additionally, we have included data pertaining the gating compliance within the gating margin. Such data is unique in the MRgRT setting.

TABLE 1 Constraints and plan quality metrics that guided planning are summarized in the first row with the individual statistics for each retrospective plan in the following rows.

Site	Degree of epidural involvement	Spinal cord D0.03 \leq 14 Gy [Gy]	Spinal cord V10Gy \leq 0.35cc [cc]	Partial spinal cord V10Gy \leq 10% [%]	V105% outside target \leq 2–3cc [cc]	D0.03 outside 1 cm \leq 18.9 Gy [Gy]	D0.03 outside target \leq 115% Rx [Gy]
C4	Epidural involvement	10.55	0.05	1.74	0.30	13.91	19.64
T7	Epidural involvement	9.10	0.00	0.00	0.62	14.00	19.79
T10	No involvement	10.40	0.07	3.35	0.02	11.00	18.62
T10	No involvement	8.93	0.00	0.00	0.42	12.35	19.74
T12	Pedicle involvement	9.47	0.01	0.54	0.31	12.76	19.94
L1	No involvement	8.86	0.01	0.13	0.10	14.05	19.36
Average \pm Standard Deviation		9.55 \pm 0.68	0.02 \pm 0.02	0.96 \pm 1.22	0.30 \pm 0.20	13.01 \pm 1.11	19.52 \pm 0.44

Tissue and coverage constraints were met, however further enhancing coverage was limited by the target hotspot and the need to keep the 115% isodose line inside the target.

Methods

Plan quality and deliverability

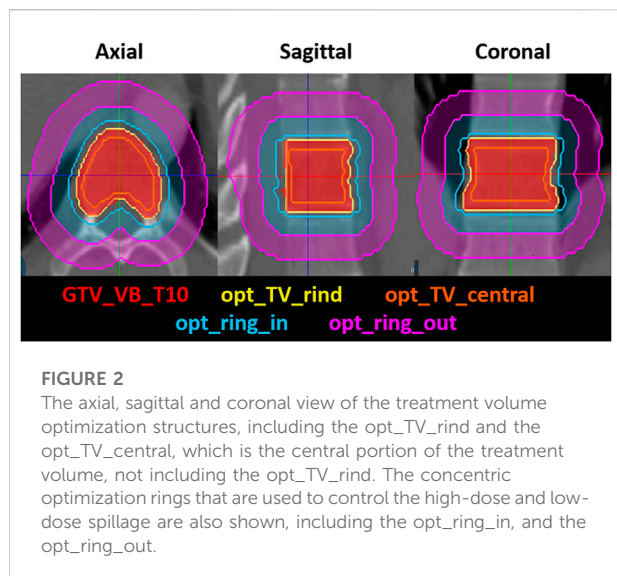
Six spine-Stereotactic Radiosurgery (SRS) patients were re-planned to 18 Gy in one fraction for a retrospective plan quality evaluation, representing the highest plan complexity for spine-SBRT. The population included one cervical, four thoracic, and one lumbar vertebral body with varying degrees of epidural and pedicle involvement. Plans were generated for the ViewRay MRIdian MR-Linac system (ViewRay Inc., Oakwood Village, OH) which combines a 0.35 T MRI system with a 6 MV flattening filter free beam delivered at a nominal dose rate of 600 MU/min. The treatment technique utilized 9–13 posterior step-and-shoot intensity-modulated radiation therapy (IMRT) beams with a double-stacked multi-leaf collimator (MLC) that can achieve field sizes down to $2 \times 4.2 \text{ mm}^2$. Dose calculation was performed by a fast Monte Carlo dose calculation algorithm, without accounting for the static magnetic field, and utilizing a 1 mm grid resolution and 1% statistical uncertainty during dose prediction. Plans were optimized to achieve coverage, constraints, and plan quality criteria recommended by RTOG 0631 for single fraction spine SBRT, included in Table 1, which follows the clinical practice observed at our institution. In addition to RTOG guidelines, two in-house plan quality constraints were adhered to: the distance to falloff to 50% of the prescription dose must be less than 4 mm and the maximum point dose (D0.03 cc) in the vertebral body must be less than 22.5 Gy (125% of the prescription dose).

Deliverability and dosimetric accuracy were evaluated for all plans via patient specific quality assurance (PSQA) measurements following the standard clinical practice at our institution for all SBRT treatments on the MR-Linac. PSQA



FIGURE 1
Blue bag immobilization device, for patient setup in head first supine position with their arms up holding onto the blue ring. Notably, the posterior coil is embedded into the blue bag for reproducible coil and patient setup.

measurements were performed, including both ion-chamber measurements utilizing an A26 MR micro ion chamber (Standard Imaging Inc., Middleton, WI) and absolute film dosimetry utilizing EBT3 Gafchromic film (Ashland, Bridgewater, NJ) in a 15 cm thick by 30 cm square Solid Water High Equivalency (Gammex Inc., Wisconsin, USA) phantom, with the chamber inserted at 7.5 cm depth along central axis. A previous study has demonstrated the negligible effects of MR exposure at 0.35 T on EBT3 Gafchromic film [18]. Point dose measurements were performed in the high-dose region while absolute film dosimetry was performed with a 3% dose difference and 1 mm distance to agreement (DTA) global gamma-analysis criterion in the steep dose gradient near the spinal cord. Additionally, the total delivery time for each PSQA delivery, from the initiation of beam on to beam off,



was manually recorded to evaluate the time required to deliver the plan.

Clinical on-line adaptive plan generation

One thoracic vertebral body patient was treated to 27 Gy in three fractions, utilizing an ART workflow. The patient was simulated in the BlueBAG BodyFIX system (BodyFix, Elekta AB) in the supine, head-first position, with their arms up. Two 12-element phased array coils were used for imaging, with the posterior coil embedded into the immobilization device, as visualized in Figure 1. The treatment-planning CT was acquired on a Brilliance Big Bore (Philips Health Care, Cleveland, OH) CT-simulation with a 2 mm slice thickness. The treatment planning MRI was acquired without motion management on the MRIdian MR-Linac using a true fast imaging and steady precession (TrueFISP) sequence acquired in 172 s with a $500 \times 450 \times 430 \text{ mm}^3$ field of view, 1.5 mm slice thickness, and $1.5 \times 1.5 \text{ mm}^2$ in-plane resolution. The co-registration between the CT-simulation and MRI-simulation in the treatment position, allows for comparable flexion of the spine to reduce registration uncertainties [6]. Contouring of the clinical target volume (CTV) and corresponding OARs was performed on the TrueFISP MRI. The CT simulation image was deformably registered to the MRI simulation image, this facilitates the ability to use the electron density information of the CT for dose calculation. Additional electron density override structures are used to account for air pockets present in the MRI simulation image.

The plan was generated with twelve posterior IMRT step-and-shoot beams utilizing target volume and ring optimization structures, modeled after our institutional standard of planning

for spine-SBRT on conventional Linacs, outlined in Figure 2. The optimization structures included three target volume structures, an “opt_TV_central”, generated with an inner margin of 5 mm from the CTV, a “TV_5 mm_OAR”, which includes the CTV within 5 mm of the spinal canal and the “opt_TV_rind”, which includes the remainder of the treatment volume. Two concentric ring structures are generated to control the high and low dose spillage, the “opt_ring_in” and the “opt_ring_out” which are rings generated with margins of 3–8 mm and 9–14 mm, respectively. This standard recipe for optimizations is included in the rules of the plan, which are formulas that can be used to automatically generate contours that may be used for planning. Additional rules in the plan included the generation of the skin, a 5 mm rind of tissue extending from the exterior surface of the patient, the spinal cord planning at risk volume (PRV), generated with a 1 mm margin from the spinal cord and the “nonCTV”, which is defined as the external border of the patient minus the target volumes. These rules are utilized in the adaptive workflow, to increase the efficiency in the generation of optimization structures used in the optimization of the adapted plan once new target volume and OAR contours have been generated for the anatomy of the day.

Additionally, efforts were made to minimize plan complexity and delivery time by limiting the number of beams and segments per beam. Doses to OARs were assessed via the dose constraints for critical organs outlined in the report of AAPM task group 101 for three fraction SBRT plans [19]. The plan generated on the simulation CT and MR images is termed the original plan and is used initially as the base plan for the calculation of the predicted dose on daily anatomy in the ART workflow. One ion chamber and two film PSQA measurements, one in the target and one in the spinal cord, were acquired in a single delivery using the same methods described in Section 2.1. To evaluate the effect of variations in the lateral position of the patient on target coverage and spinal cord dose, due the limited ability of tracking only in the sagittal plane, with no indication of left right motion, the plan was re-calculated with lateral isocenter shifts ranging from one to 3 mm in the left and right direction.

Online adaptive radiation therapy workflow

Daily anatomical changes were accounted for via re-contouring and re-planning for treatment in an on-line manner utilizing the ART workflow shown in Figure 3. The patient was setup and localized utilizing a 172 s volumetric TrueFISP MRI to account for any translational setup discrepancies. The electron density map and contours (skin, spinal canal, override volumes, external, and gating structure) were deformably registered to the daily setup MRI. The electron density override structures were reviewed and adjusted as needed to account for the variation in air pockets from the simulation

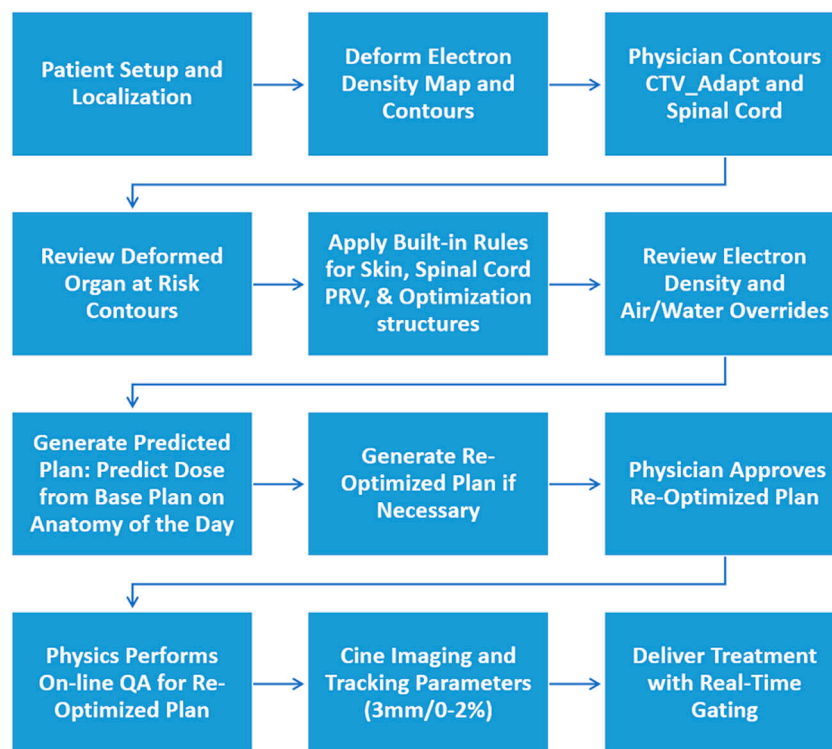


FIGURE 3
The adaptive workflow that was followed for the clinical implementation of spine SBRT.

images. The physician adjusted the CTV and spinal cord for each fraction using the daily setup TrueFISP MRI, to ensure the entire vertebral body was included in the CTV, due to the limited ability to correct for rotational setup discrepancies. The remainder of the OAR contours, including the esophagus and heart were reviewed and adjusted as needed. Rules as described in Section 2.2 were then applied. A final review of the deformed electron density map was performed due to the importance of the soft-tissue bone interface for dose calculation in the treatment area.

After the physician approval of contours, the dose from the base plan was calculated on the anatomy of the day, generating the predicted plan. Re-optimization of the predicted plan was performed to ensure that 95% of the CTV was covered with the prescription dose and that OAR dose constraints were not violated. A secondary dose calculation check of the re-optimized plan was performed with an online quality assurance (QA) tool utilizing 2%2 mm local gamma comparison. This includes a secondary Monte Carlo dose calculation comparing the original and secondary calculations via dose volume histogram and three-dimensional gamma analysis. The re-optimized beam characteristics (MU and segments) are also compared to the base plan in the online QA tool. The final physics check includes PSQA utilizing an in-

house tool, which compares the trajectory log files of the planned and delivered MLC positions.

Intrafraction image guided radiation therapy

Real-time intrafraction gating was performed utilizing single sagittal plane cine MRI images. Cine images were acquired at four frames/s with an in-plane resolution of 3.5 mm × 3.5 mm and a slice thickness of 7 mm. The surrogate structure used for real-time gating was outlined as the spinal canal. The two gating requirements include the gating margin to generate the gating boundary and percentage of the structure allowed outside the gating boundary, if more than this percentage of the structure is outside the gating boundary the beam is automatically gated off [20, 21]. The gating margin was an isotropic 3 mm expansion about the spinal canal, and the percentage of the gating structure allowed outside the boundary was selected at the time of treatment to be between zero and two percent.

To perform the gating process, the cine MR image acquired in the sagittal plane is compared to the “keyframe”, which is selected at the initiation of treatment on a pre-treatment cine MRI and describes the frame that best matches the sagittal slice

chosen for tracking from the daily volumetric image dataset. The key-frame is resampled to cine image resolution, but the contour defined on the keyframe is not resampled and stays at the resolution of the volumetric image dataset. If for instance, the in-plane resolution of the volumetric image is 1.5×1.5 mm then the keyframe contour will have this same resolution. Deformable image registration is performed between the resampled keyframe and cine image. The resulting displacement vector field (DVF) is interpolated to the resolution of the contour on the keyframe (1.5×1.5 mm in plane) and applied to the contour. Before rendering the contour on the cine image on the user interface, it is resampled to twice the resolution of the keyframe (0.75×0.75 mm in plane). The gating boundary is then compared to the deformed gating structure and if outside the boundary by the pre-determined percentage the beam is gated off, until the gating structure returns to within the gating boundary [21]. The total delivery time, defined as the time from the beginning of the very first beam to the end of the very last beam, including time required for gantry and MLC movement was automatically recorded for each treatment in the treatment summary report. This also included the beam-on time, defined as the percentage of the total delivery time when the beam is on.

Post treatment imaging

Once treatment was completed, a post-treatment MRI using a TrueFISP sequence acquired in 172 s with a $500 \times 450 \times 430$ mm³ field of view, 1.5 mm slice thickness, and 1.5×1.5 mm² in-plane resolution was acquired. This MRI was registered to the pre-treatment setup MRI to quantify positional changes between the initiation and completion of treatment. Additionally, the treatment plan was re-calculated with post-treatment imaging shifts included for each fraction to evaluate any changes in target coverage or doses to OARs.

Results

Plan quality and deliverability

IMRT plans met all critical-tissue constraints outlined in RTOG 0631 while covering 90% of the target with the prescription dose. Plan quality metrics for each individual plan are shown in Table 1. In all cases, the spinal cord was the most limiting organ, where the largest maximum point dose encountered was 10.55 Gy, which is below the 14 Gy maximum point dose criteria. Plan quality metrics from RTOG 0631 controlling hot spots and high-dose spillage (e.g., <115% permitted outside the target volume) were achieved but provided the greatest planning challenge. Efforts were made to minimize plan complexity utilizing on average 6.5 (SD = 1.6, N = 6) segments/beam, 10,716.38 MU (SD = 3,276.49 MU, N = 6)

per plan and an average delivery time of 24.58 min (SD = 8.00 min, N = 6). Optimized dose distributions for a T10 and L1 vertebral body plan are shown in Figure 4. The average difference between ion-chamber measurements and treatment planning system (TPS) calculations was 3.01% (SD = 1.70%, N = 6). Respective comparison for film measurements to TPS calculations was 96.55% (SD = 2.44%, N = 6) when employing a 3%1 mm DTA global gamma-analysis criterion.

Clinical on-line adaptive plan generation

The three-fraction spine-SBRT patient was treated using the ART workflow. The original plan generated for the patient can be seen in Figure 5. The plan met all critical-tissue constraints outlined in the report of AAPM task group 101 while covering 95% of the target with the prescription dose. The most challenging criteria to meet were the hot spot (<125% of the prescription dose) and high-dose spillage requirements (D0.03 cc outside target \leq 115% and <3 cc outside PTV receiving >105% of the prescription dose), as seen from the plan quality study. The original plan properties included 62 beam segments, 6048.5 MU with an estimated beam-on time of 10.08 min. The ion-chamber measurement was -4.14% different from the expected TPS calculation. Additionally, the target and spinal cord film 3%1 mm DTA global gamma analysis had passing results of 96.06 and 93.77%, respectively. Integrity of the plan with lateral variation showed spinal cord dose within tolerance for lateral variations up to 3 mm right, and up to 2 mm in the left direction. The largest difference observed with lateral shifts was a decrease in coverage of approximately 10 and 5%, for shifts up to 3 mm large in the left and right direction, respectively. This is likely due to the steep dose gradients present in SBRT planning.

Online adaptive radiation therapy workflow

Interfraction visibility of the spinal cord allowed for patient setup focusing on spinal cord-alignment. Daily shifts, all less than 5 mm can be seen in Table 2 for each of the three fractions. Additionally, a summary of the original, predicted, and re-optimized plans for each of the fractions can be seen in Table 3. A new re-optimized plan was generated on-line for both the first and second fractions to ensure 95% of the CTV was covered with 27 Gy. Only one re-optimization iteration, without the need to adjust the optimization cost function, was required to meet coverage constraints. The first and second fraction re-optimized plan properties included 63 and 61 beam segments, 6582.5 and 6779.7 MU and an estimated beam on time of 10.97 and 11.30 min, respectively. The adaptive QA results were 99.74 and 99.65% for fractions one and two, respectively.

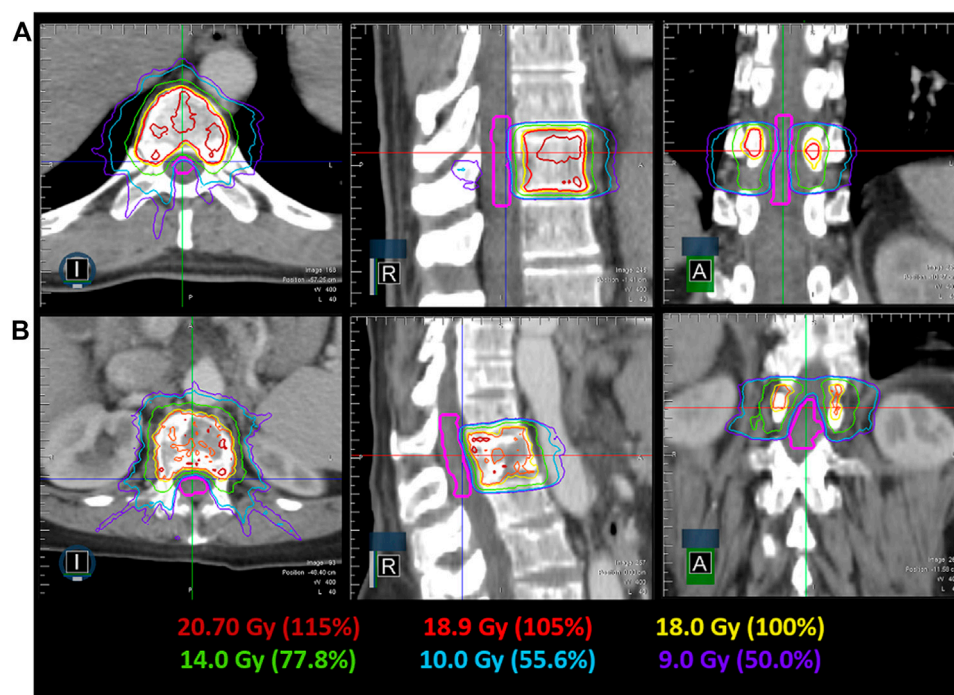


FIGURE 4

Achievable dose distribution in the axial, coronal and sagittal view for a T10 (A) and L1 (B) spine SRS plan. The spinal cord contour is shown in pink, while the relevant isodose lines are indicated by their color.

The MLC trajectory log PSQA yielded maximum root mean square error of 0.0018 and 0.0022 cm for fractions one and two, respectively, and a maximum leaf position error of 0.0100 cm and a rate of MLC position errors >0.35 cm of 0.00% for both fractions. This meets the criteria specified in the report of AAPM task group 142 [22]. For the final fraction, the adapted plan generated for fraction two was used as the base plan and proved to have sufficient coverage at the time of dose prediction on the anatomy of the day. A pre-treatment scan was used when movement was indicated via patient or sagittal cine image, to visually assess the patient position in three dimensions, after the adaptive workflow and prior to initiation of the treatment delivery. A pre-treatment volumetric image for fraction three resulted in the application of lateral and vertical shifts of 0.5 mm.

Intrafraction image guided radiation therapy

Real-time tracking and gating on a 4-frames/second sagittal MR cine image proved sufficient for intrafraction tracking of the spinal canal when a 3.0 mm gating boundary and 1–2% criteria on the gating volume excursion were utilized during treatment. The fraction one cine image can be seen in Figure 5, where an initial region of excursion allowance (ROE) of 0% was used. However, it was increased to 1% at

the beginning of treatment due to limitations in the in-plane resolution (3.5 mm \times 3.5 mm) and in the deformation of the gating structure, resulting in the gating structure artificially being pulled anteriorly. In fractions two and three a 2 and 1% ROE allowance were used for real-time gating, respectively, using the spinal canal as the surrogate gating structure. Variation in ROE was due to the qualitative assessment of the deformable registration on the sagittal cine image used for tracking on each individual fraction. The total delivery time for each fraction was 16.98, 17.38 and 17.33 min. The beam-on time was 87.2% for fraction one and 87.5% for both fraction two and three. After the definition of the gating structure and specification of the gating parameters were finalized, the structure remained within the gating parameters for the entirety of treatment.

Post-treatment imaging

Post-treatment imaging registrations to the patient initial setup scans can be seen in Table 4. Largest deviations were noted in the lateral direction. The largest vector shift was observed in the first fraction at 3.3 mm. Post-treatment dose calculations showed a decrease in coverage in the first and second fraction, with 82.8 and 90.8% of the target volume being covered with the prescription dose. Target coverage was maintained at 95.7% of the target volume receiving the prescription dose in the third

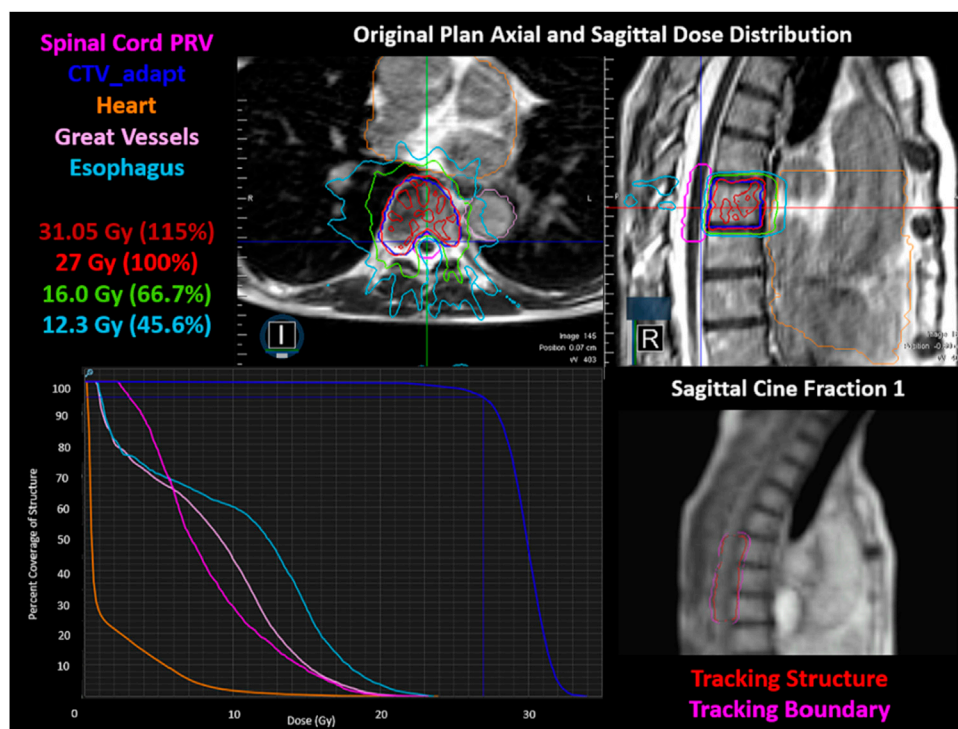


FIGURE 5
The original plan axial and sagittal dose distributions, showing the isodose lines, target structure, and organs at risk. The corresponding DVH is shown in the bottom left. The cine image quality for fraction one is shown in the bottom right, including the tracking structure in red and the tracking boundary in pink.

TABLE 2 Daily volumetric imaging shifts for the initial patient setup and pre-treatment localization images, as well as the tracking parameters used.

Fraction number	Online match (cm)			Tracking parameters (cm, %)
	Lateral	Vertical	Axial	
1 – Initial Localization	0.10	-0.15	-0.35	0.3, 0–1%
2 – Initial Localization	-0.20	0.10	0.45	0.3, 2%
3 – Initial Localization	-0.10	-0.15	-0.10	0.3, 1%
3 – Pre-Treatment	-0.05	0.05	0.00	
Average ± Standard Deviation	0.11 ± 0.05	0.11 ± 0.04	0.22 ± 0.18	

fraction. Additionally, in each of the fractions the dose to the spinal cord remained within tolerance when including the shifts from the post-treatment image.

Discussion

In spine SBRT, high-dose coverage, conformity, and spinal cord dose are critical planning characteristics. Radiation

targeting accuracy of the MR-Linac system was previously assessed via 14 end-to-end (E2E) measurements of the coincidence between the imaging, mechanical, and radiation isocenters using a Winston-Lutz technique described in a previous publication [23, 24]. This was done in order to evaluate the uncertainty in the process from simulation to image-guided localization and treatment. Assessment of the radiation targeting accuracy of the MRIdian, averaged over fourteen E2E measurements, yielded residual setup errors of

TABLE 3 Dose volume characteristics for the original plan, predicted, and re-optimized plans, if applicable for each of the three fractions delivered via the ART workflow.

Structure	Rx constraint	Orig. Plan	Day 1		Day 2		Day 3
			Predicted	Re-optimized	Predicted	Re-optimized	Predicted
CTV_adapt	≥ 95% at 27 Gy [%]	95.00	88.94	95.00	89.05	95.00	95.88
	≤ 0.03 cc at 33.75 Gy [cc]	0.03	0.11	0.04	0.13	0.04	0.13
SpinalCord PRV	≤ 0.35 cc at 18 Gy [cc]	0.07	0.10	0.13	0.09	0.05	0.20
	≤ 10% at 18 Gy [%]	1.85	2.49	3.37	2.20	1.26	5.17
	≤ 1.2 cc at 12.3 Gy [cc]	0.70	0.70	0.79	0.59	0.58	0.80
	≤ 0.03 cc at 21.9 Gy [cc]	0.00	0.00	0.00	0.01	0.00	0.02
Esophagus	≤ 5 cc at 17.7 Gy [cc]	0.71	0.28	0.40	0.93	0.65	0.48
	≤ 0.03 cc at 25.2 Gy [cc]	0.00	0.00	0.00	0.01	0.00	0.00
Heart	≤ 15 cc at 24 Gy [cc]	0.00	0.01	0.01	0.03	0.01	0.00
	≤ 0.03 cc at 30 Gy [cc]	0.00	0.00	0.00	0.00	0.00	0.00
Great Vessel	≤ 10 cc at 39 Gy [cc]	0.00	0.00	0.00	0.00	0.00	0.00
	≤ 0.03 cc at 45 Gy [cc]	0.00	0.00	0.00	0.00	0.00	0.00
nonPTV	≤ 3 cc at 28.35 Gy [cc]	1.51	1.59	1.79	1.84	1.73	1.69
	≤ 0.03 cc at 31.05 Gy [cc]	0.01	0.09	0.09	0.10	0.06	0.11

TABLE 4 Post-treatment imaging registrations with initial setup scan translational shifts. Positive shifts indicate shifts in the right, anterior and inferior direction, negative shifts indicate movement in the left posterior and superior direction.

Translational shifts (mm)

Fraction	Lateral	Vertical	Longitudinal	Vector
1	2.7	-1.8	-0.5	3.3
2	1.4	-0.9	0.3	1.7
3	1.0	0.5	-0.1	1.1

0.2 (SD = 0.4), 0.8 (SD = 0.3), 0.4 (SD = 0.3) mm in the anterior/posterior, superior/inferior and left/right direction, respectively. The vector length was 1.0 (SD = 0.1 mm), suggesting that the radiation targeting accuracy of the MRIdian is within acceptable published tolerances for safe delivery of SRS/SBRT [23].

In this study, we aimed to achieve dose distributions meeting plan quality metrics outlined in RTOG 0631. This protocol on image-guided SBRT for localized spine metastasis included dosimetric criteria specific to prescription isodose surface coverage, high-dose spillage, spinal cord dose, and low-dose spillage. In all six retrospective patient plans, we were able to achieve the required dosimetric criteria. Previous studies have assessed the feasibility of delivering high-quality spine-SBRT plans on the MRIdian through the comparison of plan quality metrics to those of VMAT plans generated using a TrueBeam

(Varian Medical Systems/Siemens Healthineers, Palo Alto, CA) system [10, 11]. These studies showed that similar target coverage and spinal cord dosimetry could be achieved. Within this study, we were able to show that the formulaic approach to planning and optimization utilizing concentric ring structures was able to achieve clinically acceptable plans that were robust to daily variations observed during daily adaptation. This enabled the use of the ART workflow to account for daily anatomical variation through re-contouring of the target and critical structures, while rules were able to recreate the formalized structures quickly and automatically for the optimization. The use of this method then reduced the need for multiple re-optimizations to generate a clinically acceptable plan, overall reducing the amount of time that the patient remains on the table throughout the ART workflow.

Unlike current x-ray-based systems that include the ability to correct for setup uncertainties via utilization of a six DoF couch, the MRIdian is limited to three DoF couch corrections due to the nature of the MRI bore shape. Therefore, during patient setup we are unable to account for rotational setup discrepancies in the pitch, roll, and yaw. In a previous study, it was shown that without the application of pitch and roll corrections, a significant reduction in PTV coverage could occur. This reduction in coverage depended on tumor shape and size, where smaller and more abnormally shaped targets resulted in a larger reduction in coverage with rotational errors [17]. Another study, simulating rotational errors in the pitch and yaw direction, indicated that rotational errors $>1^\circ$ could result in a

statistically significant drop in target coverage [16]. To reduce the possibility of inadequate target coverage due to the limited three DoF couch corrections during our clinical implementation of MR-guided spine SBRT, an ART workflow based on daily re-contouring of the target volume was developed and followed. Re-contouring the target and spinal cord daily allowed us to account for any rotational setup differences that effected the spinal cord and target position. With accurate contours, the base plan could be calculated on the daily anatomy and within the ART workflow, we were able to re-optimize and generate a new plan to ensure sufficient target coverage. Small translational shifts for initial setup highlights the robustness and repeatability of the patient immobilization and marking. Despite these minimal changes to the patient's setup and anatomy, the dose prediction of the original plan, on the image-of-the-day demonstrated an under coverage of the target volume for fractions one and two. However, due to the steep dose gradients, small changes in contour position relative to the dose may lead to large changes in target coverage.

The soft-tissue contrast achievable in MRgRT on an MR-Linac, as shown in Figure 5 and previously [10, 25], allows for patient localization focusing on the safety of the spinal cord itself. Additionally, automated beam gating during treatment delivery via single sagittal plane MR cine images, is possible on the MRIdian. Real-time anatomy tracking and beam control do have inherent spatial and temporal limitations due to the in-plane image resolution and limited 4-frames/second image acquisition [21]. The in-plane spatial resolution of the sagittal cine MRI limited the gating margin selection. Ideally, with a PRV margin of 1 mm, we would choose this as our gating margin. However, this was not achievable on the cine-based imaging due to the limited image resolution and a larger gating margin of 3 mm was required. Further improvements in the spatial resolution of MRI cine images may offer the ability to decrease the gating margin to further improve real-time gating during treatment.

Another consideration pertains to the gating latency. Research has shown that the beam off gating latency resulting from lag between actual tumor position and the beam off condition can result in underdosage of the PTV and excessive dose to normal tissues, requiring a gating margin of up to 3–4 mm [26, 27]. The diameter of the spinal canal decreases in the cranial-caudal direction as described previously [28], and also varies significantly in dimension, for example 10–20 mm the cervical region and less than 10 mm in the thoracic region [29]. This implies that the beam off latency will result in different dosimetric impact on the spinal canal at different regions of the spine, suggesting a role for variable gating boundaries for such treatments.

In our experience, the visualization of the spinal canal on MR sagittal cine imaging enabled canal based real-time gating throughout the duration of treatment in the superior-inferior and anterior-posterior directions. As the spinal cord is the most dose limiting structure in spine SBRT, the ability to track the spinal canal itself is advantageous. However, with the version of software

available at the time of delivery there was no real-time gating available in the lateral direction. This inability to account for lateral shifts during treatment delivery was of clinical concern. To possibly mitigate for any variations in patient positioning throughout the treatment delivery, a post-treatment MRI image was acquired to evaluate if any increase in dose to the spinal cord was present. If so, this could be accounted for in future fractions by further reducing the required dose tolerances. Post-treatment imaging proved spinal cord dose remained within acceptable tolerances and no further dose reduction techniques were required. However, a decrease in target coverage, below the 95% threshold was observed in the first two fractions. MRI cine real-time gating in the axial, sagittal and coronal planes available in newer versions of the delivery platform may further improve our gating capabilities in the right-left direction to ensure confidence in the accurate and precise delivery of treatment and reduce the likelihood of the decrease in coverage observed here. Additional improvements to the treatment delivery platform may help address current limitations in the delivery of MRgRT spine SBRT, which led to decreased coverage of the target volume. Specifically, pre-treatment and mid-treatment verification imaging is commonly implemented at multiple institutions [30]. The seamless implementation of volumetric imaging throughout the ART workflow or delivery process, without having to exit the treatment application, as required currently, would aid in ensuring proper patient positioning and maintenance of target coverage throughout the duration of treatment. Furthermore, it has been shown in previous studies, that a two to 3 mm margin is required to encompass the patient setup error [31, 32]. Specifically, it was found that a 3 mm margin is required when an evacuated cushion is used for immobilization [32], as was used during this study. Although our post-treatment imaging shows a decrease in coverage, the time-point that these shifts occurred is unknown as these shifts were not indicated by our real-time gating. Volumetric imaging throughout the duration of treatment, real-time gating and tracking with increased spatial resolution in all three dimensions or the use of a 3 mm margin would be beneficial to ensure target coverage.

The MRIdian MR-Linac and ART workflow offers the added benefit of soft-tissue contrast, target and critical structure re-contouring based off of daily anatomy, and target tracking and beam gating during treatment. Additional limitations include the increased treatment time associated with the step-and-shoot IMRT treatment modality, as patients undergoing spine-SBRT treatment have difficulty holding still due to substantial pain [33]. The average delivery time for spine SRS utilizing VMAT is approximately 3–9 min [11, 25]. By comparison, single fraction SRS beam-on time in this study was 24.5(SD = 5) minutes. Other similar planning studies indicate delivery times ranging from 9 to 12 min for multi-fraction treatments [10, 11]. Our multi-fraction clinical delivery had an average delivery time of 17.2(SD = 0.2) minutes. In each scenario, the beam-on time required for spine SBRT on the MRIdian is longer

than that required for VMAT treatment. This further emphasizes the importance of continued patient position verification *via* real-time cine and volumetric MR images.

Conclusion

The achieved plan quality and deliverability of six retrospectively planned spine-SRS cases and one spine-SBRT clinical case, was shown to be within acceptable clinical standards. MR-guidance with an on-line ART workflow offered increased accuracy in the localization of the spinal cord at the time of initial treatment setup, while additionally ensuring sufficient target volume coverage in the initial treatment plan itself, indicating the potential need for on-line adaptation in this treatment setting. Real-time gating of the spinal canal demonstrated patient immobilization during the MR-Linac treatment delivery, however, further improvements in the MRI cine spatial resolution and ability to gate in all three planes is necessary to maintain target coverage and ensure the accuracy and precision during the treatment of future Spine-SBRT treatments.

Data availability statement

The datasets presented in this article are not readily available because of patient confidentiality. Requests to access the datasets should be directed to the corresponding author.

Author contributions

The authors confirm contribution to the paper as follows: study conception and design: IC and JD; contributed data and clinical expertise: PP and SS; data collection: JC, JD, JK, and KCS;

References

- Husain ZA, Sahgal A, De Salles A, Funaro M, Glover J, Hayashi M, et al. Stereotactic body radiotherapy for de novo spinal metastases: Systematic review. *J Neurosurg Spine* (2017) 27(3):295–302. Epub 2017/06/10. doi:10.3171/2017.1.Spine16684
- Ryu S, Yoon H, Stessin A, Gutman F, Rosiello A, Davis R. Contemporary treatment with Radiosurgery for spine metastasis and spinal cord compression in 2015. *Radiat Oncol J* (2015) 33(1):1–11. Epub 2015/03/31. doi:10.3857/roj.2015.33.1.1
- Toussaint A, Richter A, Mantel F, Flickinger JC, Grills IS, Tyagi N, et al. Variability in spine Radiosurgery treatment planning – results of an international multi-institutional study. *Radiat Oncol* (2016) 11(1):57. doi:10.1186/s13014-016-0631-9
- Ulin K, Urie MM, Cherlow JM. Results of a multi-institutional benchmark test for cranial ct/mr image registration. *Int. J. Radiat. Oncol. Biol. Phys.* (2010) 77(5): 1584–9. doi:10.1016/j.ijrobp.2009.10.017
- Noel CE, Parikh PJ, Spencer CR, Green OL, Hu Y, Mutic S, et al. Comparison of onboard low-field magnetic resonance imaging versus onboard computed tomography for anatomy visualization in radiotherapy. *Acta Oncologica* (2015) 54(9):1474–82. doi:10.3109/0284186X.2015.1062541

analysis and interpretation of results: IC, JC, and JD; draft manuscript preparation: JC.

Acknowledgments

We are grateful to Rajiv Lotey of ViewRay for providing details pertaining to the real-time gating procedure on the MRidian machine.

Conflict of interest

JC reports travel expenses from ViewRay outside of this work. PP and JD report grants from ViewRay outside of this work. IC, PP, JD, and JK report honoraria and travel expenses from ViewRay outside of this work. JK reports travel expenses from Varian Medical Systems/Siemens Healthineers outside of this work. IC reports grants from Varian Medical Systems/Siemens Healthineers and Philips HealthCare outside of this work.

The remaining authors declare that the research was conducted in the absence of any commercial or financial relationships that could be construed as a potential conflict of interest.

Publisher's note

All claims expressed in this article are solely those of the authors and do not necessarily represent those of their affiliated organizations, or those of the publisher, the editors and the reviewers. Any product that may be evaluated in this article, or claim that may be made by its manufacturer, is not guaranteed or endorsed by the publisher.

- Spieler B, Samuels SE, Llorente R, Yechieli R, Ford JC, Mellon EA. Advantages of radiation therapy simulation with 0.35 tesla magnetic resonance imaging for stereotactic ablation of spinal metastases. *Pract Radiation Oncol* (2020) 10(5): 339–44. doi:10.1016/j.prro.2019.10.018
- Sahgal A, Ames C, Chou D, Ma L, Huang K, Xu W, et al. Stereotactic body radiotherapy is effective salvage therapy for patients with prior radiation of spinal metastases. *Int. J. Radiat. Oncol. Biol. Phys.* (2009) 74(3):723–31. Epub 2008/12/20. doi:10.1016/j.ijrobp.2008.09.020
- Ryu S, Fang Yin F, Rock J, Zhu J, Chu A, Kagan E, et al. Image-guided and intensity-modulated Radiosurgery for patients with spinal metastasis. *Cancer* (2003) 97(8):2013–8. Epub 2003/04/04. doi:10.1002/cncr.11296
- Robinson CBJ, Victoria J, Dempsey J, Mutic S, Kashani R. Comparison of spinal cord motion versus vertebral body motion during magnetic resonance imaging-guided radiation therapy (Mr-Igrrt). *Int. J. Radiat. Oncol. Biol. Phys.* (2014) 90: 301–2. doi:10.1016/j.ijrobp.2014.05.1012
- Yadav P, Musunuru HB, Witt JS, Bassetti M, Bayouth J, Baschnagel AM. Dosimetric study for spine stereotactic body radiation therapy: Magnetic resonance guided linear accelerator versus volumetric Modulated Arc therapy. *Radiol Oncol* (2019) 53(3):362–8. Epub 2019/09/26. doi:10.2478/raon-2019-0042

11. Redler G, Stevens T, Cammin J, Malin M, Green O, Mutic S, et al. Dosimetric feasibility of utilizing the viewray magnetic resonance guided linac system for image-guided spine stereotactic body radiation therapy. *Cureus* (2019) 11(12): e6364. Epub 2020/01/16. doi:10.7759/cureus.6364
12. Zeng KL, Tseng C-L, Soliman H, Weiss Y, Sahgal A, Myrehaug S. Stereotactic body radiotherapy (sbrt) for oligometastatic spine metastases: An overview. *Front Oncol* (2019)9: (337) 337. doi:10.3389/fonc.2019.00337
13. Tseng C-L, Sussman MS, Atenafu EG, Letourneau D, Ma L, Soliman H, et al. Magnetic resonance imaging assessment of spinal cord and cauda equina motion in supine patients with spinal metastases planned for spine stereotactic body radiation therapy. *Int. J. Radiat. Oncol. Biol. Phys.* (2015) 91(5):995–1002. doi:10.1016/j.ijrobp.2014.12.037
14. Oztek MA, Mayr NA, Mossa-Basha M, Nyflot M, Sponseller PA, Wu W, et al. The dancing cord: Inherent spinal cord motion and its effect on cord dose in spine stereotactic body radiation therapy. *Neurosurg* (2020) 87(6):1157–66. doi:10.1093/neuros/nyaa202
15. Maziero D, Straza MW, Ford JC, Bovi JA, Diwanji T, Stoyanova R, et al. Mr-guided radiotherapy for brain and spine tumors. *Front Oncol* (2021) 11:626100. Epub 2021/03/26. doi:10.3389/fonc.2021.626100
16. Li F, Park J, Lalonde R, Jang SY, diMayorca MS, Flickinger JC, et al. Is Halcyon feasible for single thoracic or lumbar vertebral segment sbrt? *J Appl Clin Med Phys* (2022) 23(1):e13458. doi:10.1002/acm2.13458
17. Schreiber E, Fox T, Crocker I. Dosimetric effects of manual cone-beam ct (cbct) matching for spinal Radiosurgery: Our experience. *J Appl Clin Med Phys* (2011) 12(3):132–41. doi:10.1120/jacmp.v12i3.3467
18. Khaferllari I, Kim JP, Liyanage R, Liu C, Du D, Doemer A, et al. Clinical utility of gafchromic film in an mri-guided linear accelerator. *Radiat Oncol* (2021) 16(1): 117. doi:10.1186/s13014-021-01844-z
19. Benedict SH, Yenice KM, Followill D, Galvin JM, Hinson W, Kavanagh B, et al. Stereotactic body radiation therapy: The report of aapm task group 101. *Med Phys* (2010) 37(8):4078–101. doi:10.1118/1.3438081
20. Klüter S. Technical design and concept of a 0.35 T mr-linac. *Clin Translational Radiation Oncol* (2019) 18:98–101. doi:10.1016/j.ctro.2019.04.007
21. Green OL, Rankine LJ, Cai B, Curcuru A, Kashani R, Rodriguez V, et al. First clinical implementation of real-time, real anatomy tracking and radiation beam control. *Med Phys* (2018) 45(8):3728–40. doi:10.1002/mp.13002
22. Klein EE, Hanley J, Bayouth J, Yin F-F, Simon W, Dresser S, et al. Task group 142 report: Quality assurance of medical accelerators. *Med Phys* (2009) 36(9): 4197–212. doi:10.1118/1.3190392
23. Wen N, Kim J, Doemer A, Glide-Hurst C, Chetty IJ, Liu C, et al. Evaluation of a magnetic resonance guided linear accelerator for stereotactic Radiosurgery treatment. *Radiother Oncol* (2018) 127(3):460–6. doi:10.1016/j.radonc.2018.04.034
24. Winston KR, Lutz W. Linear accelerator as a neurosurgical tool for stereotactic Radiosurgery. *Neurosurgery* (1988) 22(3):454–64. Epub 1988/03/01. doi:10.1227/00006123-198803000-00002
25. Choi CH, Park S-Y, Kim J-I, Kim JH, Kim K, Carlson J, et al. Quality of tri-Co-60 Mr-igrt treatment plans in comparison with vmat treatment plans for spine sabr. *Br J Radiol* (2017) 90(1070):20160652. Epub 2016/12/08. doi:10.1259/bjr.20160652
26. Kim T, Lewis B, Lotey R, Barberi E, Green O. Clinical experience of mri 4d quasar motion phantom for latency measurements in 0.35t mr.linac. *J Appl Clin Med Phys* (2020) 22: 128–36. doi:10.1002/acm2.13118
27. Hu P, Li X, Liu W, Yan B, Xue X, Yang F, et al. Dosimetry impact of gating latency in cine magnetic resonance image guided breath-hold pancreatic cancer radiotherapy. *Phys Med Biol* (2022) 67(5):055008. doi:10.1088/1361-6560/ac53e0
28. Ulbrich EJ, Schraner C, Boesch C, Hodler J, Busato A, Anderson SE, et al. Normative mr cervical spinal canal dimensions. *Radiology* (2014) 271(1):172–82. Epub 2014/01/31. doi:10.1148/radiol.13120370
29. Frostell A, Hakim R, Thelin EP, Mattsson P, Svensson M. A review of the segmental diameter of the healthy human spinal cord. *Front Neurol* (2016) 7:238. doi:10.3389/fneur.2016.00238
30. Guckenberger M, Sweeney RA, Flickinger JC, Gerszten PC, Kersh R, Sheehan J, et al. Clinical practice of image-guided spine Radiosurgery - results from an international research consortium. *Radiat Oncol* (2011) 6(1):172. doi:10.1186/1748-717X-6-172
31. Copeland A, Barron A, Fontenot J. Analytical setup margin for spinal stereotactic body radiotherapy based on measured errors. *Radiat Oncol* (2021) 16(1):234. doi:10.1186/s13014-021-01956-6
32. Li W, Purdie TG, Taremi M, Fung S, Brade A, Cho BC, et al. Effect of immobilization and performance Status on intrafraction motion for stereotactic Lung radiotherapy: Analysis of 133 patients. *Int. J. Radiat. Oncol. Biol. Phys.* (2011) 81(5):1568–75. Epub 2010/11/16. doi:10.1016/j.ijrobp.2010.09.035
33. Wu QJ, Yoo S, Kirkpatrick JP, Thongphiew D, Yin F-F. Volumetric arc intensity-modulated therapy for spine body radiotherapy: Comparison with static intensity-modulated treatment. *Int. J. Radiat. Oncol. Biol. Phys.* (2009) 75(5): 1596–604. doi:10.1016/j.ijrobp.2009.05.005